PROCEEDINGS of the
23rd International Congress on Acoustics
9 to 13 September 2019 in Aachen, Germany

Sensorless Measurement of the Acoustic Impedance of a Loudspeaker

Romain BOULANDET[(1)]

[(1)]HEPIA, HES-SO University of Applied Sciences and Arts Western Switzerland, romain.boulandet@hesge.ch

Abstract

This paper presents an experimental approach for estimating the front-side radiation impedance of a loudspeaker. This acoustic load impedance is the reaction of the sound field on the radiating diaphragm which may affect the loudspeaker response, particularly in the low frequencies due to the coupling with the room modes. In general, this impedance can not be solved analytically because it depends both on the physical characteristics of the speaker and the complexity of the acoustic field in which it radiates. Conventional measurement techniques require sensors such as microphones and accelerometers. The approach proposed here relies mainly on the reciprocal mechanism of electrodynamic transduction, making it possible to use the loudspeaker as a sensor simultaneously. This work shows that the front-side acoustic impedance can be derived from the speaker input impedance and the knowledge of its electromechanical parameters. An analytical model is given and data measured in actual rooms provides proof of concept. Potential applications are also discussed.

Keywords: Loudspeaker radiation impedance, Acoustic impedance meter, Sound field monitoring

1 INTRODUCTION

The complex interaction between a room and a loudspeaker is reflected by the air load on the radiating diaphragm. The real part of this acoustic impedance represents the sound power radiated into the air by the diaphragm and the imaginary part is the stored (reactive) power that is returned to the source. In general, the front-side radiation impedance depends on both the loudspeaker configuration and the characteristics of the room. The radiation impedance of a vibrating surface can be calculated in some simple configurations and analytical models can be found in [1, 2, 3]. State-of-the-art methods require sensors to measure acoustic impedance. A general literature review of measurement methods for characterizing passive acoustic components such as absorbing materials, mufflers or wind instruments can be found in [4]. An impedance sensor using an electrodynamic transducer and two microphones to produce a controlled volume velocity source is described in Ref. [5]. As shown in [5], this measurement device can be used to estimate the characteristics of the loudspeaker enclosure (eg volume size and thermal losses for a sealed enclosure, vent characteristics and Helmholtz resonance for a bass-reflex speaker). In the case of a direct radiator loudspeaker system, the front-side acoustic impedance can be measured very close to the diaphragm using a microphone and a nearby vibration sensor. Doutres *et al.* (2010) developed a methodology for determining intrinsic properties of porous samples from the measurement of the input impedance of an electrodynamic loudspeaker used to apply static and dynamic stress on it [6]. Recently, Ahadi and Bakhtiar (2014) proposed a computer-based measurement system using a similar approach to assess the acoustic impedance of a closed duct [7]. Some difficulties in applying this method are reported in [8], where suggestions for improving the range of application are made based on FEM simulation. Moreover, Boulandet *et al.* (2016) showed that the mobility characteristics of a mechanical structure can also be detected from the variations of the input impedance of an electrodynamic actuator fixed thereto [9].

In this paper, we propose a straightforward method for evaluating the front acoustic load seen by a voice coil loudspeaker operating at low frequencies. Rather than using external sensors, we propose to estimate the acoustic load impedance directly through the reciprocal electrodynamic coupling, thus using the loudspeaker as an acoustic impedance meter. The remaining is organized as follow. In Section 2, we describe how to obtain the acoustic load impedance from the loudspeaker input impedance. Section 3 describes the methodology and illustrates the performance of the concept using measured data and results computed using the finite element method. Concluding remarks are provided, discussing potential applications in actual listening rooms.

2 THEORY

This section provides the basic equations describing how to obtain the front-side acoustic load impedance of a loudspeaker without using an additional sensor. An impedance-based modelling approach is used to derive input/output relationships between variables in different parts of the loudspeaker. The lumped model discussed below is appropriate in small signal operation when the transducer behaves sufficiently linearly [10].

The governing equations of the voice coil loudspeaker can be written in the complex frequency domain as [3]

$$\begin{aligned} S_d p_1 - S_d p_2 &= Z_m(\omega)\, v + Bl\, i \\ u &= Z_e(\omega)\, i - Bl\, v \end{aligned} \tag{1}$$

where p_1 and p_2 are the acoustic pressures at the front and back of the diaphragm, respectively, v is the diaphragm velocity, i is the current flowing through the coil, Bl is the transduction coefficient, S_d is the effective piston area representing the diaphragm radiating surface, and u is the voltage at the input terminals. In Eq. (1), $Z_m(\omega) = \mathrm{j}\omega M_{ms} + R_{ms} + (\mathrm{j}\omega C_{ms})^{-1}$ is the mechanical impedance and $Z_e(\omega) = \mathrm{j}\omega L_e + R_e + \mathrm{j}\omega L_2 R_2 (\mathrm{j}\omega L_2 + R_2)^{-1}$ is the electrical impedance of the driver unit including eddy current [11]. Figure 1 gives the analogous electrical circuit representation of the loudspeaker driver mounted in a baffle, where Z_{ar1} and Z_{ar2} denote the front and the back-side acoustic radiation impedances.

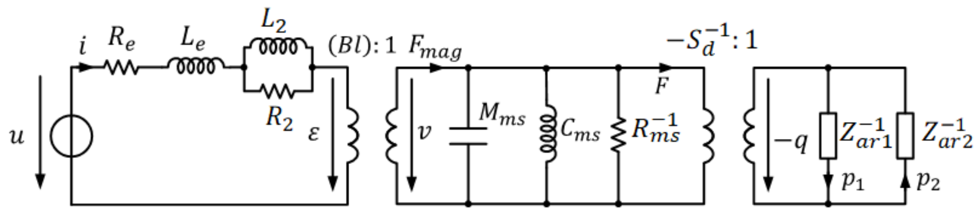

Figure 1. Equivalent circuit representation of the voice coil loudspeaker mounted in a baffle; $\varepsilon = -Blv$ is the back electromotive force, $F_{mag} = Bli$ is the magnetic force on the current-carrying wires, and q is the volume velocity.

In vacuum, i.e. $p_1 = p_2 = 0$ in Eq. (1), the speaker input impedance seen by the audio amplifier can be written as:

$$Z_{inv}(\omega) = \left.\frac{u}{i}\right|_{p_1=p_2=0} = Z_e(\omega) + \frac{(Bl)^2}{Z_m(\omega)} \tag{2}$$

In open space, the vibration of the diaphragm is influenced by the presence of air on both sides, which modifies the speaker input impedance as

$$Z_{in}(\omega) = \frac{u}{i} = Z_e(\omega) + \frac{(Bl)^2}{Z_m(\omega) + Z_{mr1}(\omega) + Z_{mr2}(\omega)} \tag{3}$$

where $Z_{mr1} = S_d^2 Z_{ar1}$ and $Z_{mr2} = S_d^2 Z_{ar2}$ denote the front and the back-side radiation impedances, respectively. As shown in Eq. (3), the acoustic load exerted by the air on both sides of the diaphragm may affect the frequency response of the loudspeaker.

From Eqs. (1-3), the transfer function between the input current and the output diaphragm velocity can be expressed as

$$G(\omega) = \frac{v}{i} = -\frac{1}{Bl}\left(Z_{in}(\omega) - Z_e(\omega)\right) \tag{4}$$

From Eqs. (3-4), and after some further manipulations, the front radiation impedance can be expressed as

$$Z_{mr1}(\omega) = -\frac{Bl}{G(\omega)} - Z_m(\omega) - Z_{mr2}(\omega) \tag{5}$$

As can be seen in Eq. (5), the front radiation impedance can be readily obtained from variations in the speaker electrical input impedance and prior knowledge of the speaker fundamental parameters. Note that Z_{mr2} is substituted with

$$Z_{mb}(\omega) = \left(\mathrm{j}\omega M_{ab} + R_{ab} + \frac{\rho c^2}{\mathrm{j}\omega V_b} \right) S_d^2 \tag{6}$$

in Eqs. (5) and (3) for a closed-box loudspeaker system, where V_b is the net enclosure volume, ρ is the density of air, c is the speed of sound in air, M_{ab} is an equivalent acoustic mass and R_{ab} an acoustic resistance [3].

3 RESULTS

This section describes the methodology used to develop the concept of sensorless acoustic load impedance meter and illustrates the overall performance under free-field conditions and in a lightly damped room. As discussed above, the approach proposed here for obtaining the front-side acoustic load at the loudspeaker diaphragm requires prior knowledge of the electromechanical parameters of the loudspeaker driver. The equivalent electrical circuit models derived in Section 2 are used in the following to find the Thiele-Small (T/S) parameters using a curve fitting method.

3.1 Evaluation of Thiel/Small parameters

The values of the T/S parameters are determined by measuring the loudspeaker input impedance, near the resonance frequency, at small signal levels for which the mechanical behavior of the driver is effectively linear (i.e., proportional to its input). Figure 2 shows the experimental setup used to evaluate the T/S parameters.

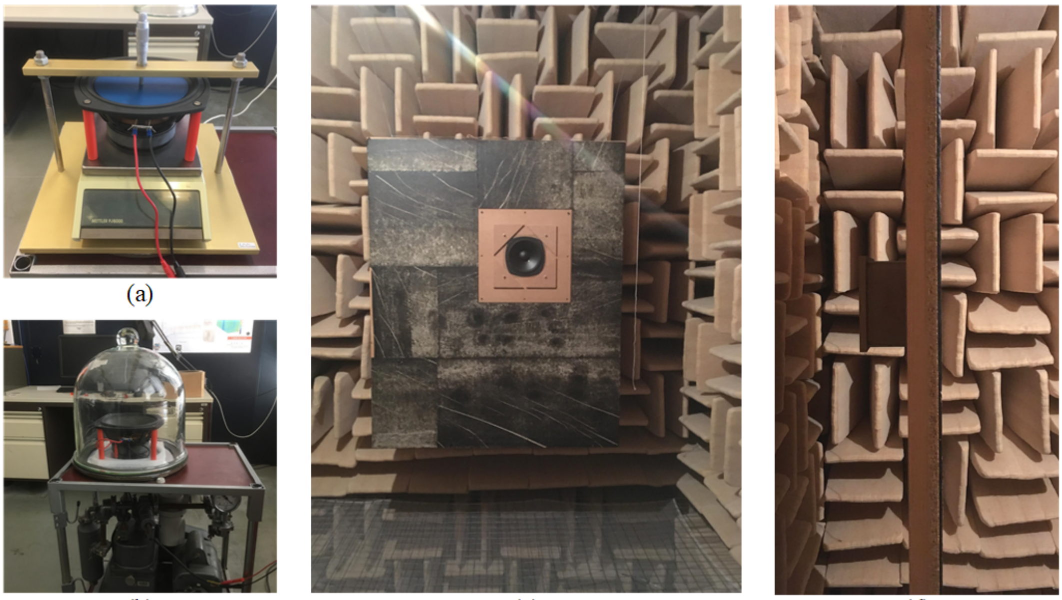

(a) (b) (c) (d)

Figure 2. Experimental setup for measurement of the electrical impedance of the loudspeaker driver (a) when the coil is blocked, (b) in vacuum, and (c) mounted in a baffle in open space. In (a), a specific locking system is used to prevent the diaphragm from vibrating, and thus the coil attached thereto; in (b), the loudspeaker driver unit is placed in a vacuum chamber to eliminate the effect of air on the diaphragm; in (c), the loudspeaker driver is mounted in a baffle in an anechoic chamber.

Figure 3 illustrates the input impedance of the loudspeaker measured and calculated for different configurations. The Matlab function lsqcurvefit was used to solve the data-fitting problems in the least squares sens. As can be seen in Fig. 3, there is a good agreement between the measured and fitted data, especially around the resonance frequency. As the frequency increases, some discontinuities in the frequency response can be observed. They are partly due to the break-up modes of the diaphragm, as shown in Fig. 3. Imperfect clamping of the coil may also explain the differences shown between the measured and fitted data in Fig. 3 (b).

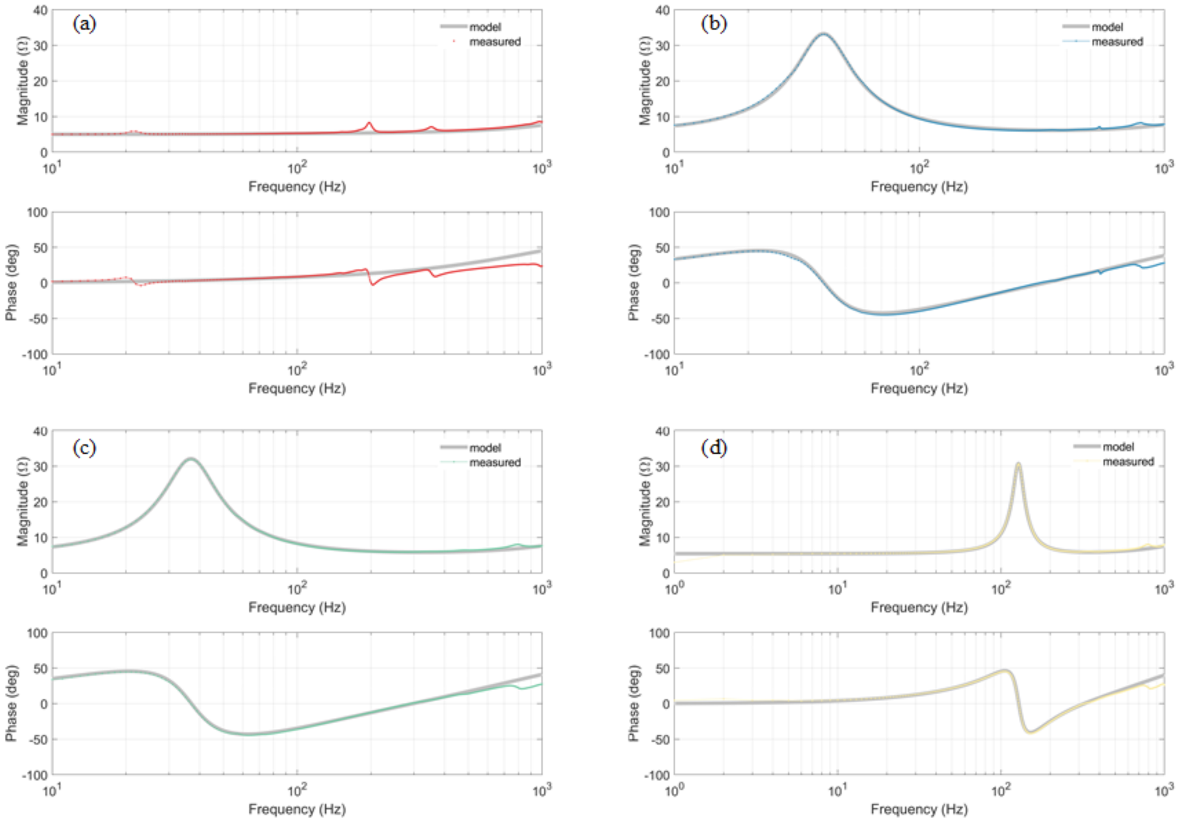

Figure 3. Measured and fitted data of the electrical impedance of the loudspeaker driver (a) when the coil is blocked, (b) in vacuum, (c) mounted in a baffle in anechoic chamber and (d) closed-box loudspeaker mounted in a baffle in anechoic chamber.

The parameters R_e, L_e, R_2 and L_2 are estimated from the speaker input impedance with the coil blocked, as shown in Fig. 3 (a), when the loudspeaker impedance only depends on the physical properties and the geometry of the coil. The parameters M_{ms}, R_{ms}, C_{ms} and Bl are estimated from the speaker input impedance in vacuum, as shown in Fig. 3 (b). As given in Eq. (2), the speaker input impedance in vacuum reveals the effect of the mechanical part in addition to that of the coil, but does not include the acoustic load exerted on the diaphragm. In free-field conditions, as given in Eq. (3), the speaker input impedance also depends on the acoustic radiation on both sides of the diaphragm. It can be seen in Fig. 3 (c) that the resonant peak is a bit lower and slightly shifted lower in frequency compared to that in vacuum. This is due to the coupling between the diaphragm and air which has the effect of adding an acoustic resistance and an acoustic mass to the loudspeaker. The parameters M_{ab}, R_{ab} and C_{ab} in Eq. (6) are deduced from the input impedance shown in Figs. 3 (c) and (d). The estimated values of the T/S parameters are summarized in Tab. 1.

Table 1. Thiele/Small parameters of the loudspeaker measured at small signal levels.

Parameter	**Notation**	**Value**	**Unit**
dc resistance of the coil	R_e	5.19	Ω
Inductance of the coil	L_e	0.78	mH
Resistance due to eddy currents	R_2	0.37	Ω
Para-inductance of the voice coil	L_2	0.38	mH
Transduction coefficient	Bl	9.3	$\mathrm{N\,A^{-1}}$
Moving mass	M_{ms}	23.7	g
Mechanical resistance	R_{ms}	3.11	$\mathrm{N\,s\,m^{-1}}$
Mechanical compliance	C_{ms}	0.646	$\mathrm{mm\,N^{-1}}$
Projected area of the diaphragm	S_d	227	$\mathrm{cm^2}$
In vacuum resonance frequency	f_s	41	Hz
Acoustic compliance of the cabinet	C_{ab}	$0.03097\,10^{-6}$	$\mathrm{m^3\,Pa^{-1}}$

3.2 Experimental proof of concept

Once the T/S parameters of the loudspeaker system have been determined, equations (4) and (5) can be used to estimate the output velocity to input current relationship and the front radiation impedance, respectively. Figure 4 shows the experimental configurations used to provide a proof of concept. A Polytec ISV-500 Laser Doppler Velocimeter is used to measure the normal velocity of the diaphragm. A Brüel and Kjaer $1/2$ inch free-field measurement microphone is used to measure the acoustic pressure. A Brüel and Kjaer LAN-XI TYPE 3160 multichannel analyzer is used to measurement. Note that the loudspeaker is driven by a voltage-controlled current source (not shown here), which is designed to simultaneously measure the current and voltage at the input terminals.

(a) (b)

Figure 4. Experimental setup for estimating the front-side acoustic load impedance on the closed-box loudspeaker system (a) placed in an anechoic room and (b) located near a corner in a lightly damped room.

Figure 5 illustrates the frequency response function between the input current and output velocity for different configurations. As can be seen in Fig. 5, there is a good agreement between the measured data and the model given in Eq. (4). For the loudspeaker used for this study, the useful frequency range extends over a decade between about 25 Hz and 300 Hz. For higher frequencies, it can be seen that the measured and estimated data are different due to unmodelled dynamics in the loudspeaker system and inaccuracies in the coil inductance estimation. It can be noted in particular in Fig. 5 (d) that room modes can be clearly distinguished from the estimated data.

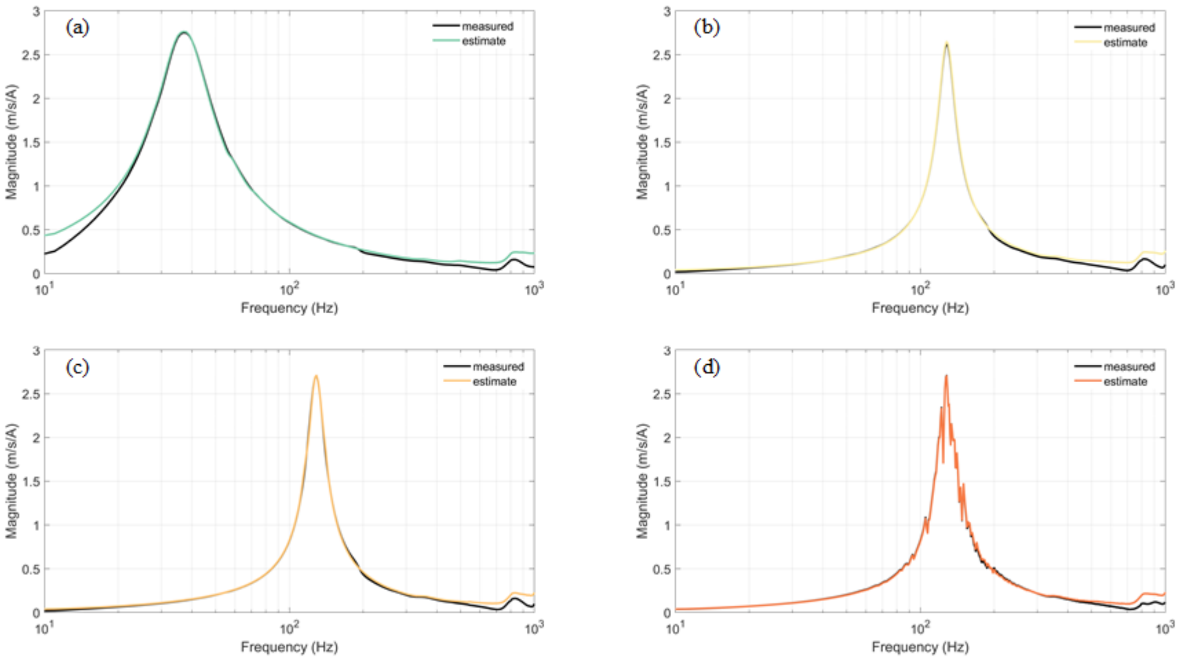

Figure 5. Frequency response function between the input current and the output velocity as given in Eq. (4) of (a) the loudspeaker mounted in a baffle in anechoic chamber, (b) the closed-box loudspeaker mounted in a baffle in anechoic chamber, (c) the closed-box loudspeaker placed in an anechoic room and (d) in a lightly damped room.

Figure 6 illustrates the frequency response function of the specific acoustic radiation impedance, i.e. the relationship between the front-side acoustic pressure and the normal velocity of the diaphragm, in different configurations. As can be seen in Fig. 6, there is a good agreement between the measured data and the model given in Eq. (5). In Fig. 6 (a), the measured and estimated data are also compared to the model of a circular piston of radius $r = 0.085$ m mounted in an infinite baffle [3]. As shown in Fig. 6 (a), the useful frequency range is larger with the baffle configuration and ranges between about 60 Hz and 300 Hz for the loudspeaker used for this study. For the closed-box configuration, the useful frequency range is from 70 Hz to 250 Hz, as shown in Figs. 6 (c) and (d). It can be noted in particular in Fig. 6 (d) that room modes can be clearly distinguished from the estimated data. As noted above, the measured and estimated data are different outside the useful frequency range due to unmodelled dynamics and inaccuracies in the coil inductance estimation.

4 DISCUSSION

As demonstrated above, the radiation characteristics of a direct-radiator loudspeaker system can be estimated with good accuracy directly through the reciprocal electrodynamic coupling. This requires monitoring both the current and voltage at the loudspeaker terminals and prior knowledge of the fundamental parameters of the loudspeaker drive unit and enclosure. The useful frequency range is, however, limited around the mechanical resonance frequency of the loudspeaker system. In particular, the break-up modes of the diaphragm, not considered in the model, can seriously affect the performance of the concept. The electronic circuit used to drive the voice coil loudspeaker while simultaneously monitoring the voltage and current at the terminals can also limit performance by disrupting the measurement of the input impedance. Compensation of the frequency response of the electronic circuit makes it possible to reduce the differences. Note that several of the Thiele/Small

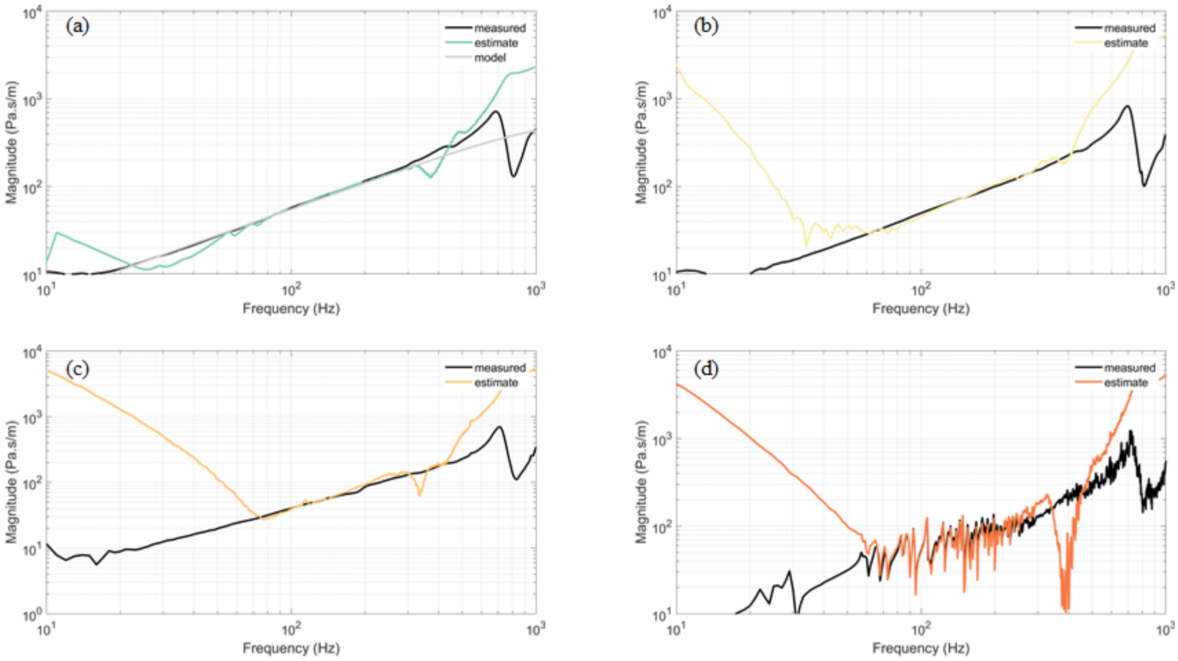

Figure 6. Frequency response function of the specific acoustic impedance (see Eq. Eq. (5)) of (a) the loudspeaker mounted in a baffle in anechoic chamber, (b) the closed-box loudspeaker mounted in a baffle in anechoic chamber, (c) the closed-box loudspeaker placed in an anechoic room and (d) in a lightly damped room.

parameters are a function of cone/voice coil excursion and therefore depend on the input voltage/current level.

5 CONCLUSIONS

This paper presents a convenient methodology to estimate the front-side radiation impedance of a voice coil loudspeaker. A lumped-parameter model is derived to obtain the acoustic load radiation characteristics of the surrounding sound field, including room modes, from a measurement of the speaker input impedance. A proof of concept is provided based on data measured in an anechoic room and in a lightly damped room. The useful frequency range is around the resonance frequency of the closed-box loudspeaker system, i.e. from about 70 Hz to 250 Hz for the loudspeaker considered in this study. The concept is able to evaluate the acoustic load exerted by the surrounding sound field on the diaphragm, especially at very low frequencies. This allows an accurate detection of the room modes that may impact the response of the speaker depending on the location in the room.

6 ACKNOWLEDGMENTS

The author wishes to thank François Bugnon for his technical assistance to the experimental configuration and Virgile Favre for his help during the measurement. The author also wishes to thank PSI Audio for providing the speakers used in this study.

REFERENCES

[1] Beranek, L.; Mellow T. Acoustics: sound fields and transducers, Academic Press, 2012.

[2] Kinsler, L. E.; et al. Fundamentals of Acoustics, 4th Edition. Wiley-VCH, 1999.

[3] Rossi, M. Audio, Presses Polytechniques Universitaires Romandes, 2007.

[4] Dalmont, J-P. Acoustic Impedance Measurement, Part I: a review, Journal of Sound and Vibration, Vol 243 (3), 2001, pp 427-439.

[5] Le Roux, J-C.; Pachebat M.; and Dalmont, J-P. A new impedance sensor for industrial applications, French Congress Acoustics 2012, Nantes, France, 2012.

[6] Doutres O.; Dauchez N.; Genevaux J-M.; Lemarquand G., and Mezil S. Ironless transducer for measuring the mechanical properties of porous materials, Review of Scientific Instrument, Vol 81, 2010 055101-8.

[7] Ahadi M.; Bakhtiar M. S. A direct method for acoustic impedance measurement based on the measurement of electrical impedance of acoustic transmitter, Applied Acoustics, Vol 77, 2014, pp 76-81.

[8] Bianco F.; Teti, L.; Licitra G.; Cerchiai M. Loudspeaker FEM modelling: Characterisation of critical aspects in acoustic impedance measure through electrical impedance, Applied Acoustics, Vol 124, 2017, pp 20-29.

[9] Boulandet R.; Michau M.; Herzog P.; Micheau P.; Berry A. A sensorless method for measuring the mobility of mechanical structure, Journal of Sound and Vibration, Vol 378, 2016, pp14-27.

[10] M. Dodd, W. Klippel, Wolfgang and J. Oclee-Brown, Voice coil impedance as a function of frequency and displacement, Audio Engineering Society Convention 117, 2004.

[11] Marshall Leach W., Loudspeaker Voice-Coil Inductance Losses: Circuit Models, Parameter Estimation, and Effect on Frequency Response, Journal of the Audio Engineering Society, Vol 50 (6), 2002, pp 442-449.